Electronic Supplementary Material (ESI) for Lab on a Chip.

Supplementary Table 1. Features and procedures of original and microbead-based SiMPull

	Original SiMPull [1,2]	**Microbead-based SiMPull** (this study)
1. Applications	Single-molecule imaging for interaction kinetics and stoichiometry; quantification of protein concentration; PPI of nonabundant proteins; rare cells	Same as original SiMPull
2. Pulldown site	Surface of glass coverslips	Surface of agarose microbeads
3. Surface passivation & functionalization	Required: PEG passivation (KOH/aminosilane used) and avidin coating	Not necessary: commercially available, pre-functionalized surface of microbeads
4. Steps/time for 3	10 steps, 6–8 h	None
5. Micro flow-chamber	Required: narrow channel between coverslip and glass slide; 0.5 h needed	Not needed: all reactions performed in 1.5-mL Eppendorf tubes
6. Difficulty of sample preparation	Difficult: micropipette used to inject solution slowly into micro flow-chamber	Easy: solution added into Eppendorf tubes
7. Total # of steps and time	21 steps 9–11 h	6 steps 2.5–3 h
8. Detection limit	~10 cells for detecting overexpressed proteins	~5–10 cells for detecting overexpressed proteins; ≤ 10 pM biotin-Atto 488
9. S/B ratio	10–20	10–20

Supplementary Figures

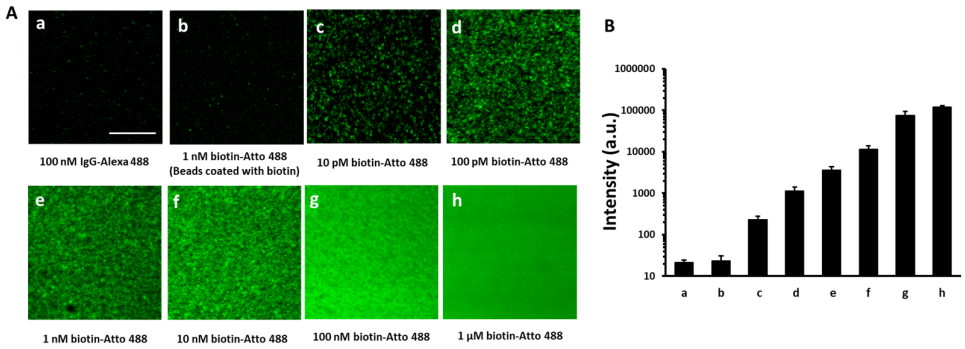

Supplementary Fig. 1. Detection sensitivity of NeutrAvidin-coated agarose microbeads for biotin-Atto 488. A) Biotin-Atto 488 at various concentrations pulled down by NeutrAvidin-coated agarose microbeads. In Image b, for the pulldown of 1 nM biotin-Atto 488, microbeads pre-exposed to 1 µM biotin for 10 min were used; little binding occurred here, suggesting minimal nonspecific binding of biotin-Atto 488 to microbeads. IgG-Alexa 488 (100 nM): another negative control (a). Shown are 25×25 µm imaging areas selected from microbeads (see additional details in Figs. 2B and 3A-D). Scale bar, 10 µm. **B)** Average signal intensity of an imaging area similar to that in Panel A in 6 randomly selected beads in the same experiment. The microbeads detected biotin-Atto 488 at a concentration as low as 10 pM with a high signal-to-background ratio (>10 relative to column b; the Y-axis is in the logarithmic scale).

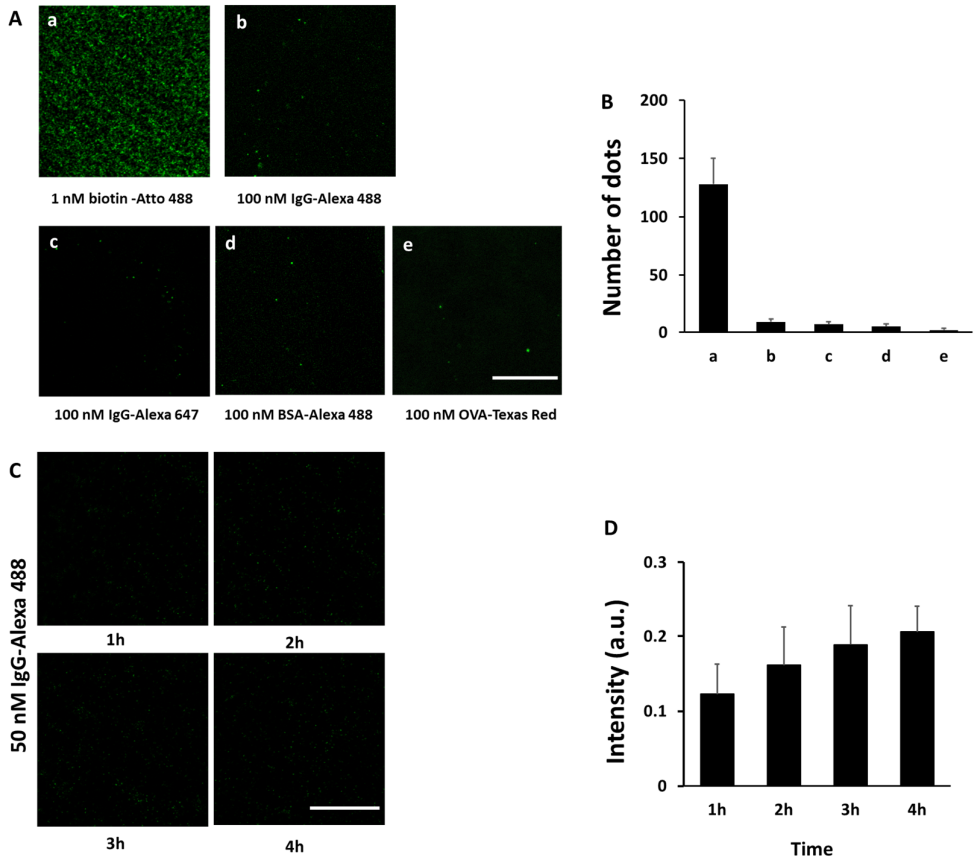

Supplementary Fig. 2. Minimal nonspecific binding of NeutrAvidin-coated agarose microbeads. A) Microbeads bound to biotin-Atto 488 (1 nM) as expected (a), but showed little binding, even at 100-fold higher concentration (100 nM), to IgG-Alexa 488, IgG-Alexa 647, BSA-Alexa 488, or OVA-Texas Red. Panels A and C show 25×25 μm imaging areas selected from microbeads (see additional details in Figs. 2B and 3A-D); scale bars, 10 μm. **B)** Average number of fluorescent dots of an imaging area similar to that in Panel A in 6 randomly selected beads in the same experiment. **C)** Time course of nonspecific binding of 100 nM IgG-Alexa 488 to microbeads. **D)** Average signal intensity of an imaging area similar to that in Panel C in 6 randomly selected beads in the same experiment.

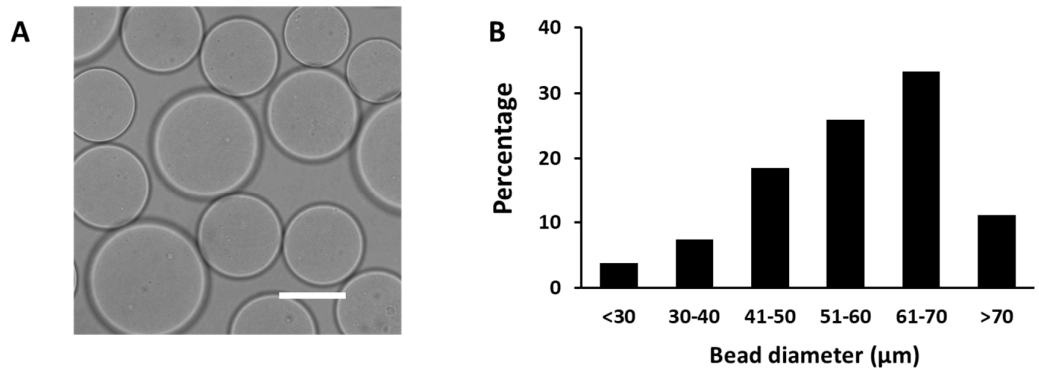

Supplementary Fig. 3. Size distribution of NeutrAvidin-coated agarose microbeads. **A)** Bright-field image of microbeads under a microscope; scale bar, 50 μm. **B)** Size distribution of a total 50 microbeads.

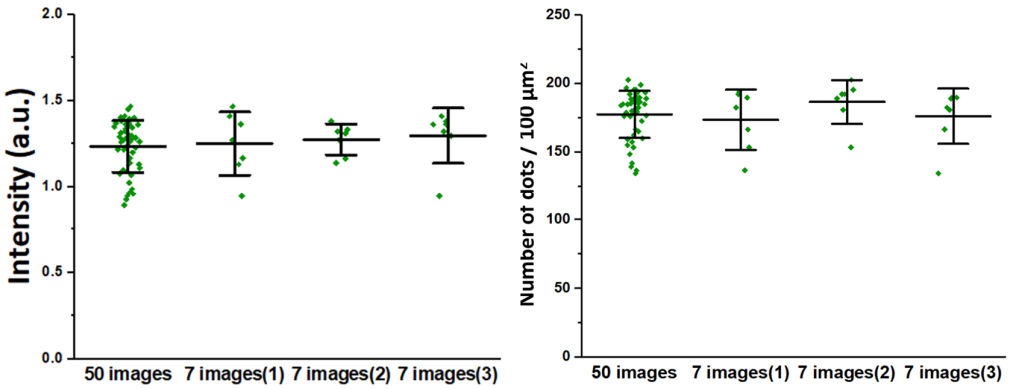

Supplementary Fig. 4. Average signal intensity of 7 microbeads faithfully represents that of 50 microbeads. The experiment here was similar to the one described in Fig. 3A-D. Fluorescent dots in a 25×25 μm imaging area were sampled from 50 randomly selected microbeads of various sizes; the average signal intensity (left) and average counts of these fluorescent dots (right) from the 50 microbeads are shown. Out of the 50 microbeads, 7 microbeads were randomly selected and the average signal intensity and average counts of the fluorescent dots on these 7 beads were compared with those of the dots on all 50 microbeads; this process was repeated thrice, and the analyses are designated in the figure as "7 images (1), 7 images (2), and 7 images (3)." The Kullback-Leibler Divergence (D_{KL}) values, a measure of dissimilarity of two probability distributions, between the average signal intensity and counts of the fluorescent dots on the 50 beads and the 7 selected beads were 0.056 and 0.101, respectively; the extremely small values of D_{KL} suggest that the measurement for the 7 microbeads faithfully represents that for the 50 microbeads, and, by extension, for all the microbeads in the experiments.

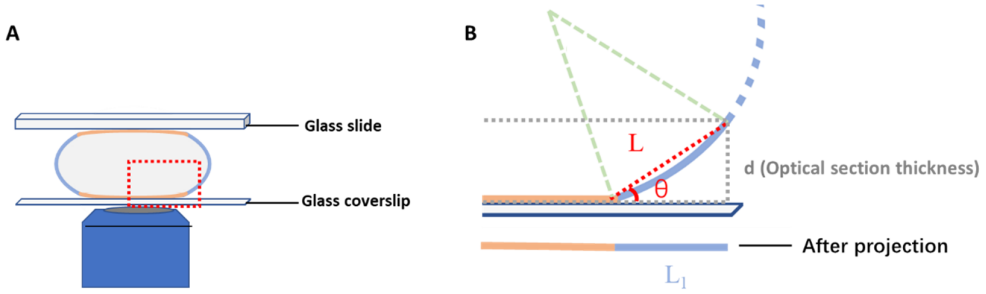

Supplementary Fig. 5. Schematic showing formation of bright aureole on agarose microbeads. **A)** Cross-section of a soft agarose microbead that is pressed and flattened between a coverslip and a glass slide. Blue object, microscope lens. **B)** Magnification of boxed area in Panel A. The red dotted line "L" is drawn to approximate the blue curved line marking the edge of the microbead, the signal on which is projected onto Line L_1. Assuming that the fluorescent signal density on the bead surface is ρ, the signal density of the orange straight line that represents the central portion of the microbead remains ρ after projection; by contrast, the signal density of the curved line (approximated by L) should be $\rho(L/L_1) = \rho/\cos\theta$ after projection. Because $\cos\theta < 1$, the signal intensity of L_1 is greater than ρ, and therefore the edge is brighter than the center (and an aureole is formed). This phenomenon is more readily observed under a low-magnification lens because such a lens (relative to a high-magnification lens) increases the optical section thickness d [3] and concurrently increases the signal density of the aureole $\rho/\cos\theta$ (by increasing θ) and L_1, the width of the aureole.

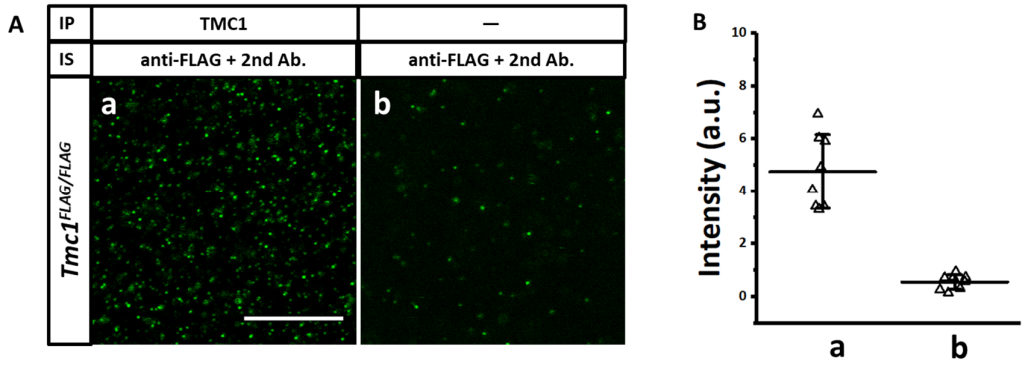

Supplementary Fig. 6. TMC1-FLAG pulldown from organ of Corti by using anti-TMC1. A) TMC1-FLAG was pulled down from tissue lysates by using anti-TMC1 and detected with anti-FLAG plus a fluorescently labeled 2nd antibody (a). Few TMC1-FLAG molecules were detected when anti-TMC1 antibody was not included in the immunoprecipitation (IP) (b, negative control). Each panel shown here is a selected (boxed) imaging area from a microbead. IS, immunostaining; scale bar, 10 μm. **B)** Statistical results of the assay in Panel A. Each triangle represents the signal intensity of one imaging area from the experiment depicted in Panel A.

SUPPLEMENTARY INFORMATION

A. Apparent number of TMC1 functional units per hair cell

The apparent number of TMC1 functional units per hair cell, N, was calculated as follows:

$$N = \frac{n_b A_b n_d}{A_i n_c}.$$

Here, n_b is the number of microbeads (100 for each experiment), A_b is the average surface area of a microbead (15,385 μm^2), n_d is the number of fluorescent dots per imaging area (350 for TMC1), A_i is the imaging area (25×25 μm^2), and n_c is the number of hair cells per experiment (2 mouse cochleae, 6,600 hair cells). We assumed that each fluorescent spot represented no more than one functional unit given the low concentration of TMC1, and we obtained an N of 130 in our experiment.

The genuine number of TMC1 functional units per hair cell could be at least 4 times higher—TMC1 pulldown and identification involved 4 layers of interactions between the 1st and 2nd antibodies and TMC1, even when we exclude the extremely tight NeutrAvidin/biotinylated-2nd-antibody interaction (see Fig. 1); this translates into only 25% of the total TMC1 molecules being captured and identified even if the efficiency at each layer of interaction is as high as 70%.

The number of TMC1 subunits in each functional unit has not been established. Dimer formation has been suggested by initial cryo-EM data and homology modeling [4,5], and the existence of tetramers is another possibility (see below).

B. Fraction of total TMC1 molecules in MT complex

The proportion of total TMC1 molecules in the MT complex, P_{MT}, is calculated as follows:

$$P_{MT} = \frac{N_{MT}}{N_{total}}$$

N_{MT} and N_{total}: number of TMC1 functional units in the MT complex of the hair bundle and in the entire cell, respectively.

The results of recent photobleaching experiments conducted by Beurg et al. suggested that a single MT complex contained 8–20 TMC1 subunits in a tonotopic gradient[6]. The findings suggest that TMC1 could function as a dimer or tetramer if not a monomer, and this implies that each MT complex harbors an average of 7 (for dimer) or 3.5 (for tetramer) functional units. Because a single hair cell contains ~70 stereocilia in total and two-thirds of these (in the two shorter rows out of the three rows of stereocilia in total) contain a single MT complex, each hair cell contains ~45 MT complexes and therefore 315 (for tetramer) or 158 (for tetramer) TMC1 functional units, which is the value of N_{MT}.

N_{total} is the genuine number of TMC1 functional units per hair cell, which could be 4 times the N value (see above); this yields an N_{total} of 520 and thus a P_{MT} of 30%–60%.

Reference

1 A. Jain, R. Liu, B. Ramani, E. Arauz, Y. Ishitsuka, K. Ragunathan, J. Park, J. Chen, Y. K. Xiang and T. Ha, Nature, 2011, 473, 484–488.

2 A. Jain, R. Liu, Y. K. Xiang and T. Ha, Nat. Protoc., 2012, 7, 445–452.

3 T. WILSON, J. Microsc., 2011, 244, 113–121.

4 A. Ballesteros, C. Fenollar-Ferrer and K. J. Swartz, Elife, 2018, 7: e38433.

5 B. Pan, N. Akyuz, X. P. Liu, Y. Asai, C. Nist-Lund, K. Kurima, B. H. Derfler, B. György, W. Limapichat, S. Walujkar, L. N. Wimalasena, M. Sotomayor, D. P. Corey and J. R. Holt, Neuron, 2018, 99, 736-753.e6.

6 M. Beurg, R. Cui, A. C. Goldring, S. Ebrahim, R. Fettiplace and B. Kachar, Nat. Commun., 2018, 9, 1–15.